

## **NOTICE CONCERNING COPYRIGHT RESTRICTIONS**

This document may contain copyrighted materials. These materials have been made available for use in research, teaching, and private study, but may not be used for any commercial purpose. Users may not otherwise copy, reproduce, retransmit, distribute, publish, commercially exploit or otherwise transfer any material.

The copyright law of the United States (Title 17, United States Code) governs the making of photocopies or other reproductions of copyrighted material.

Under certain conditions specified in the law, libraries and archives are authorized to furnish a photocopy or other reproduction. One of these specific conditions is that the photocopy or reproduction is not to be "used for any purpose other than private study, scholarship, or research." If a user makes a request for, or later uses, a photocopy or reproduction for purposes in excess of "fair use," that user may be liable for copyright infringement.

This institution reserves the right to refuse to accept a copying order if, in its judgment, fulfillment of the order would involve violation of copyright law.

## Fracture Permeability Evolution in Rock from the Desert Peak EGS Site

Steven R. Carlson<sup>1</sup>, Jeffery J. Roberts<sup>1</sup>, Russell L. Detwiler<sup>1</sup>, Elizabeth A. Burton<sup>1</sup>,  
Ann Robertson-Tait<sup>2</sup>, Christy Morris<sup>3</sup> and Paul Kasameyer<sup>1</sup>

<sup>1</sup>Lawrence Livermore National Laboratory, Livermore, California

<sup>2</sup>GeothermEx, Inc., Richmond, California

<sup>3</sup>ORMAT Nevada Inc., Reno, Nevada

### Keywords

Fracture permeability, resistivity, Desert Peak, EGS

### ABSTRACT

Fluid flow experiments are being conducted on quartz monzonite core retrieved from depths of about 1 km at the Desert Peak East EGS site in Churchill County, Nevada. The experimental goals are to observe the evolution of fracture permeability at geothermal pressure and temperature conditions and to elucidate the controlling mechanisms. The experiments are conducted at a confining pressure of 5.5 MPa, pore pressures of 1.38 MPa or 2.07 MPa and temperatures of 167-169°C. Saline water is flowed through an artificial (saw-cut) fracture at a constant rate of 0.02 ml/min over a period of several weeks, interspersed with shorter intervals in which flow is either stopped or varied up to 2.0 ml/min. Inlet and outlet pore pressures and electrical resistance are measured throughout the experiments. Evidence for permeability evolution is provided by changes in differential pore pressure at constant flow and by changes in effective hydraulic aperture calculated from the variable flow rate data. Electrical resistance measurements provide evidence of ongoing geochemical reactions that alter fracture permeability over time. The early experiments have shown a decline in hydraulic aperture in at least one specimen. Electrical resistivity is observed to rise during flow and fall during no-flow intervals, reflecting changes in the ionic content of the pore fluid.

### Introduction

The successful development of Enhanced Geothermal Systems (EGS) depends on the creation and maintenance of permeable fractures at depth in order to extract heat efficiently and economically. Operational procedures will be influenced by the many mechanisms that control fracture permeability over time, including mineral dissolution and precipitation, chemistry effects, flow rates and stress environment. An ef-

fective EGS program will require the ability to predict the evolution of fracture permeability and to evaluate alternative operational strategies for maintaining and enhancing fracture permeability. Our goal is to elucidate these mechanisms by performing fracture permeability evolution experiments on rocks from the Desert Peak EGS site. The work consists of laboratory experiments designed to assess the evolution of permeability and geochemical attributes of induced fractures in geothermal environments under a few sets of expected conditions within the engineered reservoir, and using geochemical modeling to extrapolate those results to a broader range of expected conditions.

LLNL has developed a laboratory system to measure electrical properties of core samples to temperatures of 200°C and to confining pressures of 10 MPa. The system has been used to identify resistivity signatures of boiling in intact and fractured samples from geothermal fields (Roberts *et al.*, 2001; Detwiler *et al.*, 2003) and has since been modified to measure permeability. The laboratory measurements will be combined with geochemical modeling and chemical analyses of the effluent in order to assess permeability evolution quantitatively on artificial and natural fractures in geothermal core as a function of effective stress, fluid chemistry, and temperature. The short-term goal of these experiments is to separate the physical and chemical effects that lead to fracture permeability evolution, and to identify conditions under which permeability will be enhanced or reduced. The long-term goal is to provide quantitative values for input parameters used by coupled numerical codes to model the evolution of fracture permeability.

The Desert Peak East EGS Project is an industry-DOE sponsored effort to investigate the technical feasibility of creating an artificial geothermal reservoir east of the Desert Peak geothermal field in the Hot Springs Mountains, Churchill County, Nevada. An overview of the project is provided in Robertson-Tait and Morris (2003). If the results of the feasibility analysis are favorable, a major goal of the project will be to stimulate a hot, tight hole (DP 23-1) located about 2 km east of the producing wells. The hydraulic stimulation effort is supported by injection tests (Sanyal *et al.*, 2003), a detailed

borehole fracture analysis (Robertson-Tait *et al.*, 2004) and mechanical and other tests on core specimens retrieved from hole 35-13 TCH, located 2.4 km northeast of borehole DP 23-1. In this paper, we report initial experiments on core provided by ORMAT from the Desert Peak EGS site.

## Methods

### Specimen Preparation

The sample materials are quartz monzonite cores retrieved at depths of 1194 m and 1210 m from borehole 35-13 TCH. The specimen mineralogy consists of 44% plagioclase, 23% potassium feldspar, 7% quartz and 3% mica (Lutz, 2003). The rock contains numerous, sealed fractures in-filled with secondary minerals such as kaolin (6%), calcite (4%), and dolomite (4%). Sample porosities, calculated from the dry and saturated specimen weights, are about 2%. This value is likely an upper bound on the porosity as the measurements include microcracks induced by cooling and stress release upon retrieval from depth. A more complete geologic description of rock samples from boreholes DP 23-1 and 13-35 TCH is provided by Lutz *et al.* (2003).

Flow measurements in these experiments are made through artificial fractures. The fractures are prepared by cutting core sections along their long axes with a Mettler AE240 water-cooled rock saw. The sections are fitted back together, and two sub-cores, centered over the saw-cut, are cored from each section. The sub-cores are right circular cylinders, 25.4 mm in diameter and 43.2 mm in length, bisected by a planar saw-cut. One saw-cut surface of each specimen is bead blasted with 70-140 grit glass beads, and the other surface is hand lapped with 320-400 grit. Using this technique to fabricate fractures yields several advantages: the fracture surfaces have similar initial roughness, facilitating comparison between different experiments; small geochemical alterations of the non-bead-blasted surface can be detected, and the configuration of each sample is the same, facilitating experimental set-up. The fracture surfaces are photographed with an optical microscope at 6.3x and 20x. Portions of one fracture surface have been imaged with a scanning electron microscope.

A vacuum saturation technique is used to saturate the specimens with a dilute saline solution similar in salinity to the produced reservoir fluid. Planned experiments include a more complicated injection fluid chemistry, including dissolved silica and the use of a contacting stylus profilometer to record fracture surface topography, which will allow high-resolution quantitative measurements of the physical alteration of the rock surfaces.

### Experimental Apparatus

The test specimens are jacketed in 1-mm thick Viton tubing and fitted with Hastelloy C endcaps. The inlet endcap contains a narrow reservoir designed to distribute fluid uniformly along the upstream edge of the fracture. Care is taken to align the reservoir with the fracture. The outlet endcap contains a series of concentric channels to collect fluid over the entire surface at the downstream specimen end. Two perforated platinum disks contact the ends of the cylindrical test specimen and serve as electrodes. Thin mica inserts provide electrical insulation between the endcaps and the mounting frame, which provides a small end load to the sample.

The test specimen is inserted into an externally heated, hydrostatic pressure vessel (Figure 1). Dow Syltherm 800 heat transfer fluid is used as the confining medium. Confining pressure is supplied by an APCS pump and measured with a pressure transducer. Three Yokogawa temperature controllers control four resistance heaters placed on the outside of the pressure vessel. Confining fluid temperature is measured by a type-T thermocouple near the specimen. The pore fluid lines are 1.59 mm diameter Hastelloy tubing. The inlet line is arranged in a loop to allow the upstream fluid to attain the same temperature as the rock specimen before entering the fracture. Fluid enters the specimen at the lower end and flows upward through the fracture.

The pore fluid, which is also used to saturate the specimens, is prepared by adding 8.5g/l of high-purity NaCl to de-ionized water. The solution has an electrical conductivity of 13.75 mS/cm at room temperature. The saline solution is de-aerated for approximately 20 minutes before being introduced into the upstream reservoir. The pore fluid supply is controlled by two Isco 500D syringe pumps capable of controlling either fluid pressure or flow rate. The upstream and downstream pore fluid pressures are measured individually, and the pressure difference between the upstream and downstream reservoirs is measured with a Validyne DP 215-50 differential pressure

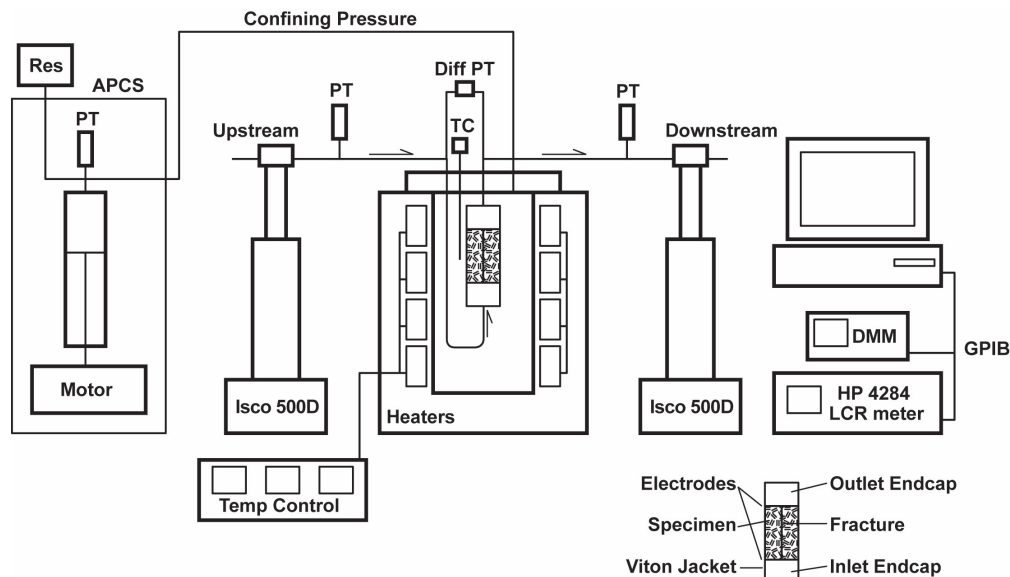


Figure 1. Schematic diagram of the experimental apparatus and specimen assembly.

transducer. A single specimen, DP 3916, was tested before the Validyne differential pressure transducer was added to the system.

The pressure transducer and temperature voltages are read with an Agilent 34970A digital multimeter. Resistance measurements are made at 100 Hz, 1 kHz and 10 kHz with an HP 4284 LCR meter. Data acquisition is controlled by National Instruments LabVIEW software on an Apple microcomputer. The APCS and Isco syringe pumps are also under computer control.

## Procedures

All flow tests to date have been conducted at a constant temperature of 167-169°C and 5.5 MPa confining pressure. In the usual, constant-flow mode of operation, the downstream syringe pump controls fluid pressure at either 1.38 or 2.07 MPa and the upstream syringe pump controls flow rate at 0.02 ml/min. The upstream syringe pump continually adjusts inlet reservoir pressure to maintain a constant flow rate through the fracture. Changes in differential pressure between the inlet and outlet reservoirs provide evidence of permeability change in the fracture over time.

We quantify permeability changes by calculating the effective hydraulic aperture of our specimen over time. The hydraulic aperture is the spacing between two parallel smooth plates that would yield the experimentally observed relationship between pressure gradient and flow rate. Though the hydraulic aperture does not account for possible changes in the roughness of the fracture surfaces, it does provide a reasonable first-order estimate of the changes caused by geochemical alteration of the fracture surfaces. At selected times, the flow rate is varied from 0.0 to 2.0 ml/min and differential pressures are recorded over five minute intervals at each flow rate. The differential pressures are divided by the specimen length to give pressure gradients. The flow rates are plotted against pressure gradients, and the slope of the linear portion of the plot is used to calculate effective hydraulic aperture,  $b$ , as

$$b^3 = 12\mu QL/(W\Delta P) \quad (1)$$

where  $\mu$  is the dynamic viscosity of water,  $Q$  is the volumetric flow rate,  $W$  and  $L$  are the fracture width and length, respectively, and  $\Delta P$  is the pressure difference across the specimen. The dynamic viscosity of water at 167°C and 2.0 MPa pressure is obtained by linear interpolation of tabulated data given in Clarke (1966). The Reynolds number,  $Re$ , is calculated as

$$Re = Vb\rho/\mu \quad (2)$$

where  $V$  is the average fluid velocity (flow rate/cross-sectional area) and  $\rho$  is density. As before,  $b$  is the effective hydraulic aperture and  $\mu$  is dynamic viscosity.

Electrical resistance is measured throughout the experiment. Flow is interrupted at selected times for periods of three to six days so that electrical resistance can also be measured under no-flow conditions. Electrical resistance is strongly sensitive to the presence of dissolved ions in the pore fluid. Observed changes in resistance over time provide evidence for active mineral dissolution and precipitation processes in the

fracture. Electrical resistivity is calculated from the measured resistances and the specimen geometry.

## Results

### Fracture Permeability

We have completed experiments on two samples thus far, DP 3916 and DP 3972.2, and testing of a third specimen, DP 3972.1, is underway. The first two experiments met with mixed success, but they have provided valuable information used in the experimental design and test protocol. Sample DP 3916 served as the initial shakedown experiment, lasting 44 days (41 days of flow) before jacket failure. Jacket failure occurred in specimen DP 3972.2 after 38 days. Differential pressure measurements were not made on specimen DP 3916, and no trend over time was observed in the differential pressure data for specimen DP 3972.2. The failure to observe a clear trend in the differential pressure data may have resulted from an overly large initial fracture aperture. A simple calculation based on equation (1) shows that changes in differential pressure are quite sensitive to the initial fracture aperture. If the initial fracture aperture is 20  $\mu\text{m}$ , 5  $\mu\text{m}$  of closure can be expected to produce only a 0.2 kPa increase in differential pressure given our specimen geometry. However, if the initial aperture is 10  $\mu\text{m}$ , only about 0.5  $\mu\text{m}$  of closure is needed to produce an equivalent pressure increase.

A clear, upward trend in differential (upstream minus downstream) pore pressure was observed during periods of constant fluid flow for specimen DP 3972.1 (Figure 2). Differential pore pressure rose 2.5 kPa during the first flow interval between Day 5 and Day 28. The sharp break in the upward trend on Day

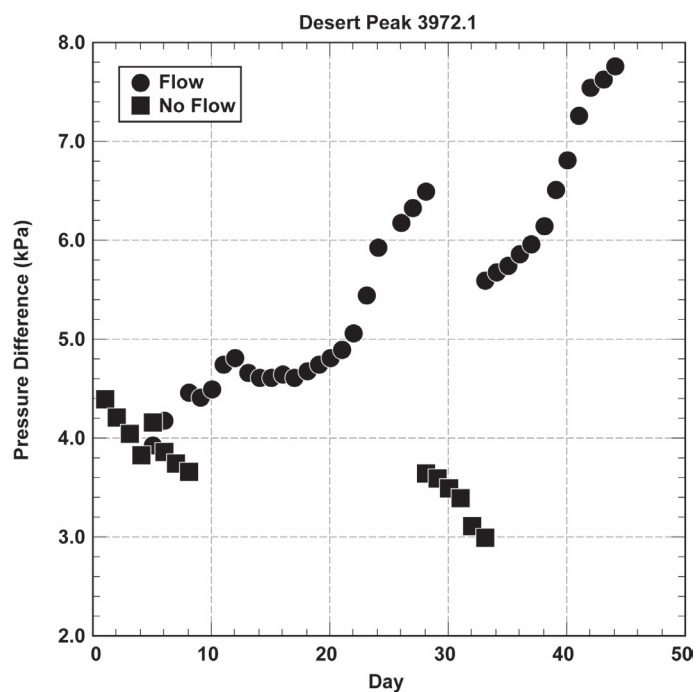


**Figure 2.** Differential Pressure (upstream minus downstream) across Specimen DP 3972.1 during constant flow (circles) and no-flow intervals (squares). Plotted points are daily averages.

28 is due to the cessation of flow. Flow was resumed on Day 33 and differential pore pressure rose a little over 2 kPa by Day 45. The overall increase in pore pressure is about 4 kPa. The increased differential pressure indicates a drop in fracture permeability because flow rate is held constant. 3972.1, Differential pore pressure fell several tenths of a kilopascal during the no-flow intervals, possibly due to instrument drift.

Effective hydraulic apertures were calculated for specimens 3972.1 and 3972.2 by regressing flow rates against pressure gradients for three variable flow rate data sets (Table 1). An effective hydraulic aperture of 18.6  $\mu\text{m}$  was obtained for specimen DP 3972.2 using flow rates up to 0.2 ml/min. The variable flow rate data for specimen DP 3972.1 are shown in Figure 3. An effective hydraulic aperture of 14.2  $\mu\text{m}$  was obtained for this specimen on Day 5 prior to flow, and a smaller aperture of 9.0  $\mu\text{m}$  was obtained for the same specimen four weeks later, on Day 33, after three weeks of flow. The loss of 5  $\mu\text{m}$  in aperture is consistent with the observed 1.6 kPa increase in differential pressure between Day 5 and Day 33 shown in Figure 2. Given an initial aperture of 14  $\mu\text{m}$ , equation (1) predicts that 5.5  $\mu\text{m}$  of closure will produce a 1.6 kPa rise in differential pressure.

A Reynolds number of 0.64 was calculated at the 0.2 ml/min flow rate using equation (2) for an aperture of 18.6  $\mu\text{m}$  and a fluid density of 0.90  $\text{g}/\text{cm}^3$  determined from tabulated pressure-volume-temperature data for water (Kennedy and Holser, 1966). This suggests that we observed linear Darcy flow even at the maximum flow rate used in the effective hydraulic aperture calculation.

**Resistivity**

Electrical resistance measurements were made throughout the experiments, and the 1 kHz resistance data were converted

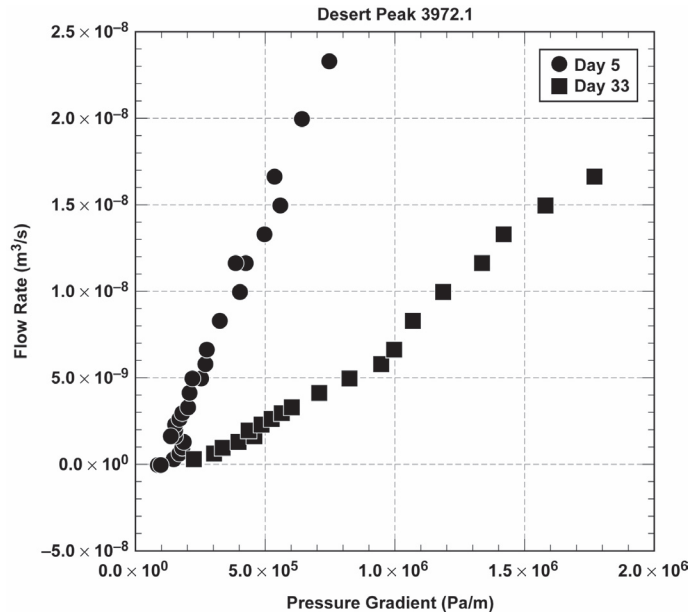


**Figure 3.** Volumetric flow rate versus pressure gradient for specimen DP 3972.1 before flow (Day 5) and after three weeks of constant flow at 0.02 ml/min flow (Day 33).

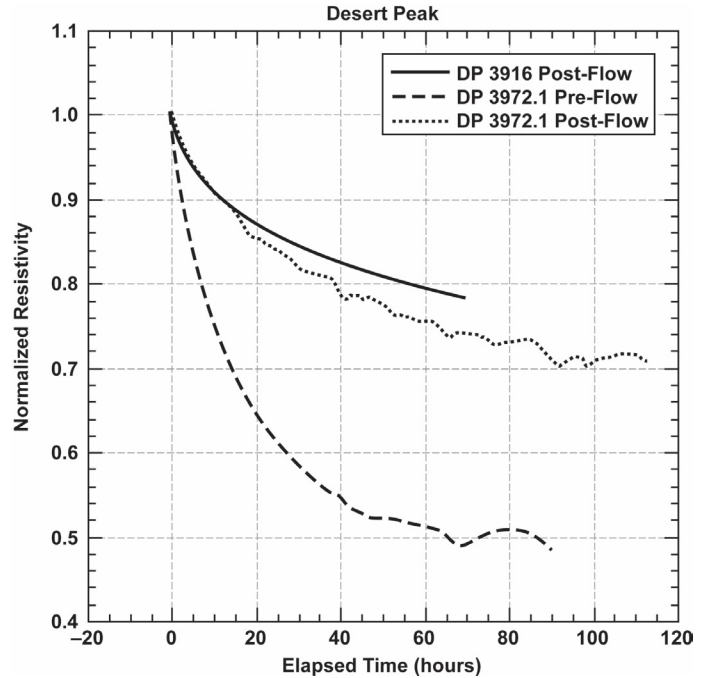


**Figure 4.** Normalized resistivity during no-flow intervals for specimens DP 3916 and DP 3972.1. Resistivity dropped at a faster rate when pore fluid made contact with fresh fracture surfaces (Pre-Flow) than with fracture surfaces that had previously been exposed to flow (Post-Flow).

to resistivity based on the cylindrical specimen geometry rather than the fracture geometry. The specimen resistivities show distinctly different trends during the constant-flow and no-flow intervals: rising during flow and falling when flow is stopped. Poor quality data were obtained during no-flow intervals for specimen DP 3972.2, but good data were obtained for specimens DP 3916 and DP 3972.1 during three no-flow intervals (Figure 4). For specimen DP 3916, flow was halted for 70 hours after 16 days of flow. Specimen DP 3972.1 was monitored under no-flow conditions for approximately one week prior to flow (Pre-Flow) and again beginning on Day 27 after about three weeks of flow (Post-Flow). The specimens remained saturated and at constant temperature during these times.

Normalized resistivity fell at a diminishing rate in each of the no-flow intervals. A drop in resistivity of about 50% was observed during the Pre-Flow interval for specimen DP3972.1, roughly twice that observed in no-flow intervals after either specimen undergone 16-32 days of flow. The larger Pre-Flow response is attributed to pore fluid contact with relatively fresh, unreacted rock surfaces. The fall in resistivity during no-flow intervals is interpreted as evidence that mineral dissolution is releasing ions into the pore fluid, providing additional charge carriers. Much of the Desert Peak quartz monzonite is composed of potassium feldspar and plagioclase, and has natural fracture fills containing carbonate minerals. Chemical reactions between these minerals and water release a number of cations that would increase the ionic conductivity of the pore fluid. Preliminary calculations demonstrate that reasonable amounts of mineral dissolution and consequent changes in fluid composition would produce a resistivity change within the

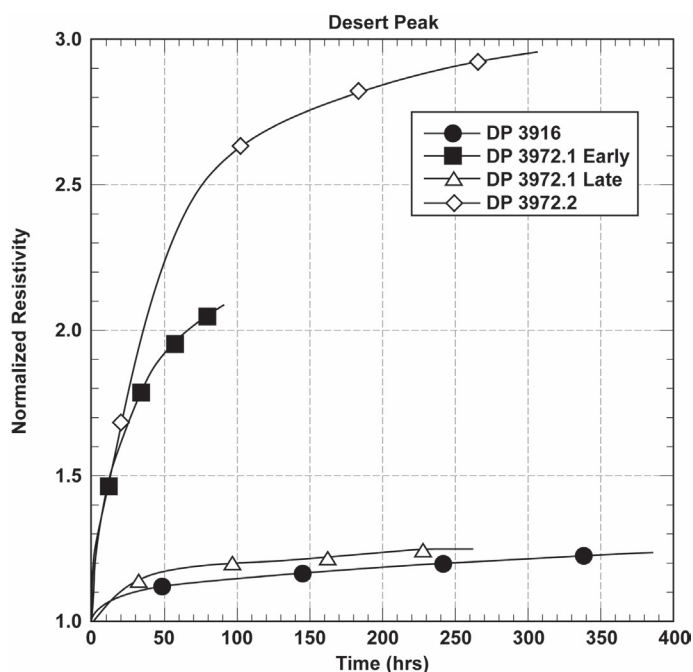


**Figure 5.** Normalized resistivity during constant flow intervals for three Desert Peak specimens. Resistivity rose during flow by as much as a factor of three.

scale of the measured change during sample shut-in. Previous experimental studies have documented dissolution of calcite, quartz, biotite, potassium feldspar and plagioclase mineral grains (e.g., Moore *et al.*, 1983; Savage *et al.*, 1992; Azaroual and Fouillac, 1997; Plagnes *et al.*, 2000; Polak *et al.*, 2003)

Electrical resistivity was observed to rise monotonically over time during constant flow for all specimens (Figure 5). Relatively large increases in resistivity were observed for specimen DP3972.2 and during the earlier of two constant-flow intervals for specimen DP 3972.1. In both cases, the constant-flow interval followed an initial, no-flow interval of several days in which resistivity dropped by as much as 50%. The other two constant flow intervals show much smaller increases in resistivity. The interval for specimen DP 3916 consists of the first 16 days of the experiment; there was no initial no-flow period. The late constant-flow interval for specimen DP 3972.1 followed a no-flow interval, shown as the dotted line in Figure 4, in which resistivity fell at a relatively slow rate.

## Conclusions

The experiments are at an early stage. The differential pressure measurements indicate that fracture permeability of core from the Desert Peak EGS site is changing in response to fluid injection. For one sample, DP 3972.1, pressure difference during constant flow at 166°C approximately doubled in 45 days. An effective hydraulic aperture of 18.6  $\mu\text{m}$  was calculated for specimen DP 3972.2. The effective hydraulic aperture for specimen DP 3972.1 fell from 14.2  $\mu\text{m}$  prior to flow to 9.0  $\mu\text{m}$  after about three weeks of flow. Electrical resistivity

**Table 1.** Effective hydraulic aperture from variable flow rate tests.

Specimen	Day	Flow Rates (ml/min)	Slope ( $\times 10^{15}$ )	Hydraulic Aperture ( $\mu\text{m}$ )	Error* ( $\mu\text{m}$ )
DP 3792.1	5	0.1 – 0.9	32.75	14.2	0.11
DP 3792.1	33	0.02 – 0.4	8.22	9.0	0.08
DP 3792.2	37	0.0 – 0.2	72.75	18.6	0.17

\*Calculated from the standard error of the linear regression slope.

measurements of the core during the experiments have proven to be a sensitive indicator of changing fracture attributes and fluid ionic content. The electrical resistance measurements show that fluid resistivity rises (conductivity falls) during flow and falls during no-flow intervals. The fall in resistivity changes during the no-flow intervals is attributed to a rise in ionic content of the pore fluid due to mineral dissolution. The fall in resistivity during flow may result from the loss of ions downstream (and out of the specimen) or from precipitation along the fracture surfaces.

These preliminary experiments form the basis for a more focused effort to understand the effects of temperature and injection fluid chemistry on changing fracture permeability. Future experiments will include more detailed study of the fluid geochemistry and mineral dissolution and how the fracture aperture is affected in an EGS environment.

## Acknowledgements

D. Ruddle and W. Ralph prepared the samples and provided valuable technical assistance. S. Fletcher provided essential technical support. The cooperation of ORMAT and GeothermEx is gratefully acknowledged. This work was supported by the Office of Geothermal and Wind Technology, under the Assistant Secretary for Energy Efficiency and Renewable Energy of the U.S. Department of Energy, and the Office of Basic Energy Science, and was performed by University of California Lawrence Livermore National Laboratory under Contract W-7405-Eng-48.

## References

- Azaroual, M and C. Fouillac, 1997. "Experimental Study and Modeling of Granite-Distilled Water Interactions at 180°C and 14 Bars." *Applied Geochemistry*, v. 12, p. 55-73.
- Clarke, S. P. Jr., 1966. "Viscosity" in Clarke, ed., *Handbook of Physical Constants*, Geol. Soc. Am. Memoir 97, Section 12, p. 291-300.
- Detwiler, R. L., J. J. Roberts, W. Ralph, and B. P. Bonner, 2003. "Modeling Fluid Flow and Electrical Resistivity in Fractured Geothermal Reservoir Rocks." *Proceedings, Twenty Eighth Annual Stanford Geothermal Reservoir Engineering Workshop, January 27-29, Stanford, CA*, SGP-TR-173, p. 301-306.
- Kennedy, G. C. and W. T. Holser, 1966. "Pressure-Volume-Temperature and Phase Relations of Water and Carbon Dioxide," in Clarke, ed., *Handbook of Physical Constants*, Geol. Soc. Am. Memoir 97, Section 16, p. 371-383.
- Lutz, S. J., 2003. "Summary of X-ray Diffraction Analysis." Energy & Geoscience Institute, University of Utah, Feb., 2003, 2 pp.

- Lutz, S. J., A. Schriener, Jr., D. Schochet, and A. Robertson-Tait, 2003. "Geologic Characterization of Pre-Tertiary Rocks at the Desert Peak East EGS Project Site, Churchill County, Nevada." *Geothermal Resources Council Transactions*, v. 27, p. 865-870.
- Moore, D. E., C. A. Morrow, and J. D. Byerlee, 1983. "Chemical Reactions Accompanying Fluid Flow Through Granite Held in a Temperature Gradient." *Geochimica et Cosmochimica Acta*, v. 47, p. 445-453.
- Plagnes, V., I. Matsunaga, M. Azaroual, H. Tao, and K. Fujimoto, 2000. "Granite-Saline Fluid Interactions in a Dynamic Experimental System at 200°C and 50 Bars." *Proceedings, World Geothermal Conference 2000, Kyushu-Tohoku, Japan May 28 – June 10, 2000*, p. 3829-3834.
- Polak, A., D. Elsworth, H. Yasuhara, A. S. Grader, and P. M. Halleck, 2003. "Permeability Reduction of a Natural Fracture under Net Dissolution by Hydrothermal Fluids." *Geophysical Research Letters*, v. 30, p. 2020-2024.
- Roberts, J. J., A. G. Duba, B. P. Bonner, and P. Kasameyer, 2001. "Resistivity During Boiling in the SB-15-D Core from The Geysers Geothermal Field: The Effects of Capillarity." *Geothermics*, v. 30, p. 235-254.
- Robertson-Tait, A. and C. Morris, 2003. "Progress and Future Plans at the Desert Peak East EGS Project." *Geothermal Resources Council Transactions*, v. 27, p. 871-877.
- Robertson-Tait, A., S. J. Lutz, J. Sheridan, and C. Morris, 2004. "Selection of an Interval for Massive Hydraulic Stimulation in Well DP 23-1, Desert Peak East EGS Project, Nevada." *Proceedings, Twenty-Ninth Workshop on Geothermal Reservoir Engineering, Stanford University*, v. 29, p.
- Sanyal, S. K., J. W. Lovekin, R. C. Henneberger, A. Robertson-Tait, and P. J. Brown, 2003. "Injection Testing for an Enhanced Geothermal System Project at Desert Peak, Nevada." *Geothermal Resources Council Transactions*, v. 27, p. 885-891.
- Savage, D., K. Bateman, and H. G. Richards, 1992. "Granite-Water Interactions in a Flow-Through Experimental System with Applications to the Hot Dry Rock Geothermal System at Rosemanowes, Cornwall, U.K." *Applied Geochemistry*, v. 7, p. 223-241.